Multi-objective System Optimization of Suborbital Spaceplane by Multi-fidelity Aerodynamic Analysis

Shintaro Tejika, Takahiro Fujikawa, and Koichi Yonemoto

Abstract An effective approach has not been established for the reusable launch vehicle, particularly for spaceplanes, whereas the conceptual design method has been established to some extent for aircraft. Spaceplanes that have wing like airplanes flight various environment, and the airframe and trajectory design problem are closely linked. Therefore, the multidisciplinary optimization method is required to optimize the airframe and the flight trajectory design at the same time in the spaceplane conceptual design. Due to computational cost constraints, a low-accuracy Computational Fluid Dynamics (CFD) method was used in a previous study to evaluate the aerodynamic characteristics of the airframe. This has been a source of concern regarding the accuracy of optimization calculations. In this study, a multi-fidelity approach is applied where the low fidelity and high-fidelity CFD are used in a complementary way. This surrogate model was connected into the manned spaceplane's Multidisciplinary Design Optimization (MDO) framework. As the load limit was reduced, the wing area grew larger and the initial mass increased.

Keywords Multidisciplinary design optimization · MOEA/D · Surrogate model · Multi-fidelity · Suborbital spaceplane

1 Introduction

It is well understood in the design process of aerospace vehicles that the quality of the conceptual study and conceptual design at the start of the process has a significant impact on the overall design, manufacturing, and operation costs. While the conceptual design method has been established to some extent for aircraft, an effective approach has not been established for reusable launch vehicles, especially for spaceplanes. Spaceplanes flight various environment, and the airframe and trajectory design problems are closely linked. Furthermore, due to the strict weight feasibility of space transportation systems, optimization techniques must be used in their design.

S. Tejika (✉) · T. Fujikawa · K. Yonemoto
Tokyo University of Science, Yamazaki 2641, Noda, Japan
e-mail: 7521536@ed.tus.ac.jp

S. Lee et al. (eds.), *The Proceedings of the 2021 Asia-Pacific International Symposium on Aerospace Technology (APISAT 2021), Volume 1*, Lecture Notes in Electrical Engineering 912, https://doi.org/10.1007/978-981-19-2689-1_21

Therefore, the MDO method is required to optimize the airframe and the flight trajectory design at the same time in the spaceplane design. Because the spaceplane MDO problem is multi-objective and multi-modal, stochastic optimization is promising. Due to computational cost constraints, a low-accuracy CFD method was used in a previous study [1] to evaluate the aerodynamic characteristics of the airframe.

Considering this issue, we focused on a multi-objective optimization algorithm using a surrogate model, which replaces a high-cost evaluation of the objective function with a surrogate model to search for good individuals. The surrogate model typically requires training data representing several input–output relationships, and after training, the estimated value of the objective function can be calculated using simple algebraic computation, enabling a much lower computational cost than CFD analysis. A multi-objective optimization algorithm that proceeds with the search while creating a surrogate model in the optimization loop is generally called Efficient Global Optimization (EGO) [2]. Since Jones et al. reported in 1998, research on EGO algorithms has been actively reported, and they have attracted attention for the ability to reduce the computational cost of optimization calculations. Among them, MOEA/D-EGO [3], a method that applies the concept of EGO to MOEA/D [4] has shown promise as a multi-objective optimization method.

In this paper, as a preliminary step to implementing EGO in MDO, outside of the optimization loop, a surrogate model is created, and a multi-objective optimization using MOEA/D is applied to a suborbital spaceplane problem and its performance is validated.

2 Aerodynamic Calculation Methods

In this study, a surrogate model is used for estimating aerodynamic characteristics, which will be discussed in Sect. 3, and various types of training data can be introduced. It is explained how to calculate high-accuracy and low-accuracy aerodynamic data to be used as training data.

2.1 Low-Accuracy Aerodynamic Calculation Method

The panel method was used for low-accuracy CFD. The panel method obtains information on velocity and pressure distribution primarily from panel data on the aircraft surface, without the use of a spatial grid, and aerodynamic force is obtained by integrating the pressure distribution. In this paper, a newly developed unstructured panel code is used for the analysis. The code is a significant extension of CPanel [5] and is based on linear potential flow theory with the Prandtl–Glauert modification [6] for subsonic speeds, and the modified Newtonian method [7] for supersonic and hypersonic speeds. The modified Newtonian method [7] and the Prandtl–Meyer expansion flow theory are used for supersonic and hypersonic flows. The van Driest II method

Table 1 Analysis conditions of FaSTAR

Velocity	Subsonic	Supersonic	Hypersonic
Domination equation	Full Navier Stokes equation		
Turbulence model	SA-noft2-R	SA-noft2-R	SA-noft2-R
Scheme for advection term	SLAU	HLLE	HLLE
Time integration method	LU-SGS	LU-SGS	LU-SGS
Slope limiter factor of N.S. equation	Quadratic	Quadratic	Linear
Slope limiter factor of turbulence model	Quadratic	Quadratic	Linear
Reconstruction method	MUSCL	MUSCL	MUSCL

for calculating frictional drag [8] and an empirical model for calculating base drag [9] have also been implemented.

2.2 High-Accuracy Aerodynamic Calculation Method

HexaGrid, an automatic grid generation tool, was used as a computational grid generation tool. We used this tool because it can generate hexahedron-based unstructured grids using only STL data from the target geometry and input parameters, and it is scalable to automatic processing. In this study, I use Fast Aerodynamic Routines (FaSTAR), a fast fluid analysis tool developed by Japan Aerospace Exploration Agency (JAXA), as a high-accuracy aerodynamic calculation method. FaSTAR is a three-dimensional compressible fluid analysis solver for unstructured meshes that is especially useful for aircraft and spacecraft aerodynamic analysis.

Table 1 shows the calculation method for each velocity. For the advection term, SLAU, in the subsonic region, a scheme corresponding to full velocity is used. The turbulence model SA-noft2-R eliminates the ft2 term involved with the trip in the Spalart–Allmaras model [10] and replaces it with the rotation correction [11].

3 Surrogate Model

3.1 Multi-fidelity

In multi-fidelity, not only conventional data with high computational cost and high accuracy can be used as training data, but also data with low computational cost and low accuracy, lowering the computational cost even further. The Co-Kriging model [12] is used in this paper.

The Co-Kriging model is an extension of the Kriging model to multiple input variables; it allows estimation using multiple training data that are correlated with

each other, rather than with one type of training data as in the Kriging model. For more information on kriging, the reader may wish to consult [13] or [14]. Two kinds of sample points must be prepared: one for the high-accuracy function and one for the low-accuracy function. It is preferable to set the sample points to cover the design variable space to prevent convergence to wrong local solutions. Because Co-Kriging model is based on the difference between high and low accuracy, the high-accuracy sample points should be included in the low-accuracy sample points so that the difference can be calculated.

3.2 Surrogate Model for Aerodynamic Analysis

This section discusses the surrogate model for estimating aerodynamic characteristics in a MDO, including the method of construction and the model's accuracy. Co-Kriging is used as a stand-in model.

3.2.1 Surrogate Model Building Method

As training data, I prepared 150 low-accuracy data and 2 high-accuracy data. For each individual, only static design variables related to the airframe shape described in Fig. 1 were generated using the Latin Hypercube method, and these data were trained to construct the surrogate model. Each individual's aerodynamic coefficients were calculated for a total of 27 cases in which the Mach number was 0.3, 0.6, 0.7, 1.5, 2.0, 3.0, 4.0, 5.0, and 10.0 [−] and the angle of attack was varied in three patterns of 0, 10, and 20 [deg.], respectively. Required time to prepare the 150 low-fidelity and 2 high-fidelity training data is 90 h. However, once the data is prepared, the time required to calculate the aerodynamic characteristics of one individual was approximately 4 min using a desktop computer (CPU: Intel Core i7-9700) for the low-accuracy CFD and

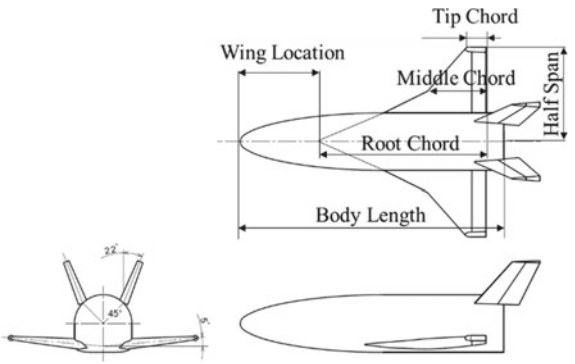

Fig. 1 Airframe shape of HIMES and variables

approximately 40 h (not including the waiting time for processing) using the JAXA supercomputer system for the high-accuracy CFD.

In this paper, the shape of the airframe is based on the WSV C-5 of the Highly Maneuverable Experimental Space (HIMES) flight vehicle [15], which was studied at ISAS/JAXA, and the variables are the body length, wing root-chord length, wing middle-chord length, wingtip chord length, and half span length. The tail wing's shape was modified from rectangular to NACA0012. Rectangular airfoils have typically been used for supersonic flight because of their good steering effect. However, there is almost no air at the altitude at which the spaceplane enters the supersonic region, and it is expected that the airfoil will be ineffective in cutting the steering surface. The front and rear positions of the wing are adjusted to match the aerodynamic center position of HIMES.

The HIMES shape was preferred as a starting point because it is designed for stability and maneuverability from subsonic to hypersonic speeds and is intended to be a practical spaceplane in the future. It is also possible to use data of wind tunnel test results obtained in the past as aerodynamic characteristics.

In this paper, OpenVehicle Sketch Pad (OpenVSP) is adopted as the software for modeling the 3D shape and generating the surface grid necessary for CFD analysis.

3.2.2 Evaluation

To determine whether the accuracy of the surrogate model has improved, the aerodynamic characteristics of the HIMES geometry with a body length of 11.5 [m] were compared. The panel method, a low-accuracy aerodynamic calculation method, and FaSTAR, a high-accuracy aerodynamic calculation method, were used to compare the aerodynamic characteristics of the HIMES shape. In Figs. 2 and 3, the shapes of high-accuracy data are represented. Figures 4 show the results of evaluating the aerodynamic data of the HIMES geometry using the low-accuracy and high-accuracy aerodynamic calculation methods and the multi-fidelity surrogate model. Despite the fact that the error is large in the subsonic region with a high angle of attack, there is an improvement in accuracy in both the subsonic and supersonic regions when

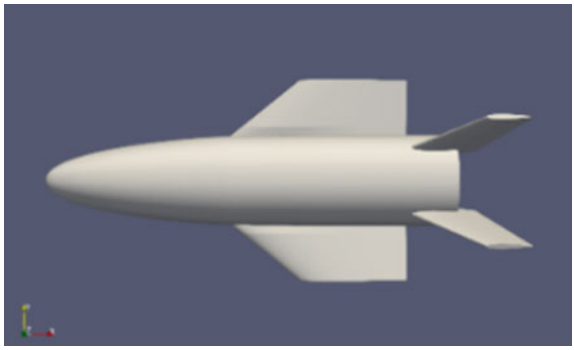

Fig. 2 The airframe of high-accuracy data 01

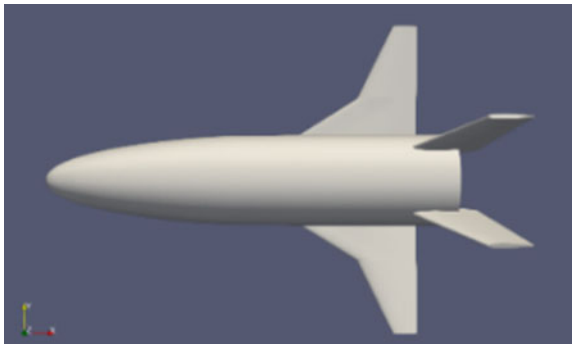

Fig. 3 The airframe of high-accuracy data 02

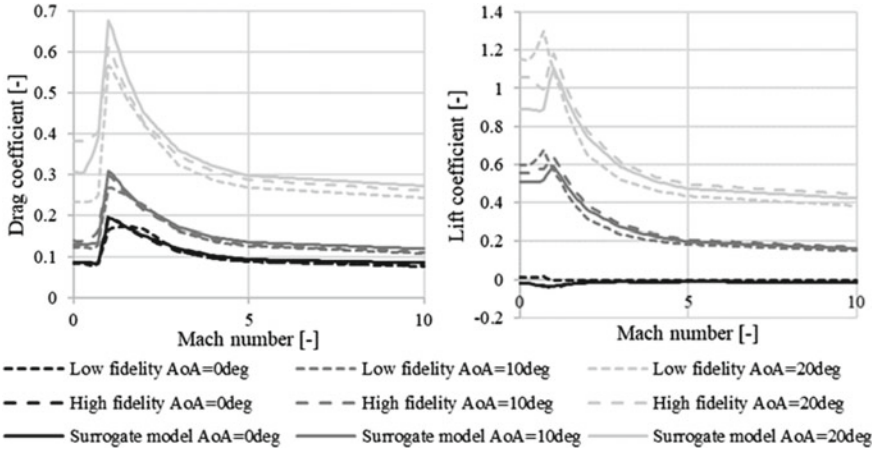

Fig. 4 Surrogate model vs. High-accuracy CFD vs. Low-accuracy CFD for drag and lift coefficient

compared to the low-accuracy aerodynamic calculation method, regardless of the fact that only two high-accuracy individuals were trained. Furthermore, the lift coefficient's peaks were consistent. Although accuracy verification was done only at one point, it was considered sufficient as a stage before EGO implementation and integrated into the analysis model.

4 MDO of Suborbital Spaceplane with the Surrogate Model

The mission is to return to the launch site after reaching an altitude of 120 km with six crew members, including passengers. The rough flight sequence is shown in Fig. 5. The following is the aircraft's assumed concept:

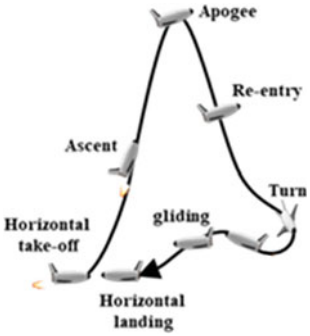

Fig. 5 Flight sequence

- It will be a completely reusable single-stage vehicle with a horizontal launch and landing.
- Multiple LOX/LNG engines are installed in a vehicle.

4.1 Design Optimization Methodology

Using the evolutionary computation method and the gradient method, I generated an optimization problem for a manned suborbital spaceplane based on the previous study [1]. The objective function of the optimization is to minimize the total mass of the aircraft at launch and the maximum load factor during flight. The variables to be optimized are shown in Table 2. The optimization problem is formulated in

Table 2 Design variables of suborbital spaceplane optimization

Category		Variable	Unit
Vehicle design	Airframe	Body length	[m]
		Root-chord length	[m]
		Middle-chord length	[m]
		Tip-chord length	[m]
		Half span length	[m]
		Main wing location	[m]
		Maximum operating load factor	[G]
		Maximum operating dynamic pressure	[Pa]
		Initial thrust-to-weight ratio desired	[−]
	Engine	The nozzle expansion ratio of engines	[−]
Trajectory	Powered ascent	State variables, Control variables, Thrust-cutoff time	
	Coasting ascent	State variables, Control variables, Apogee time	
	Nose-first return	State variables, Control variables, Return time	

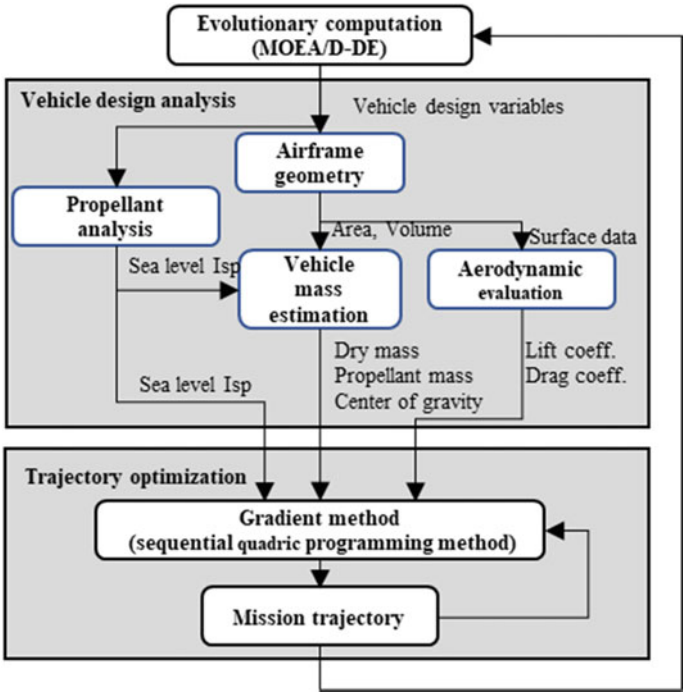

Fig. 6 Flow of optimization

this section using the framework shown in Fig. 6, and the analysis procedure is as follows.

1. In the external optimization loop, the airframe design variables in Table 2 are optimized by MOEA/D-DE [16]. The airframe design variables are input into numerical models and an airframe design analysis is performed in the individual evaluation of MOEA/D-DE. The masses and center of gravity of the airframe components are output by inputting the airframe data and the flight load conditions. These masses are added together to obtain the dry mass of the aircraft. In addition, the following constraints on the airframe design are evaluated, and when all of them are satisfied, it proceed to the next process. If any conditions are not satisfied, the individual will be regenerated.

   Constraint 1: The engine must fit in the fuselage base plane.

   Constraint 2: The trailing edge of the main wing fits into the fuselage base plane.

   Constraint 3: The thrust-to-weight ratio at lift-off is greater than 1.

   Constraint 4: The thrust-to-weight ratio at lift-off is less than 2.5.

   The result of airframe design analysis is passed to the trajectory optimization. The flight trajectory design variables in Table 2 are optimized using the

gradient method in the internal optimization loop. The objective function is to maximize the amount of propellant remaining at the time of return to the launch site. However, until the 10th generation, the evaluation in the internal loop didn't take into consideration the calculation's stability. This section's trajectory optimization problem is divided into three phases: (1) powerd ascent, (2) coasting ascent, and (3) return. The state variables include altitude, longitude, latitude, velocity, residual propellant mass, path angle, and flight heading angle. The control variables consist of the angle of attack, bank angle, and throttle opening.

2. The residuals of the following flight trajectory constraints are returned to MOEA/D-DE as the results of individuals evaluation based on the results of the flight trajectory optimization. Constraint 5: The residual propellant level at the end of Phase 3 is greater than or equal to zero. The initial and end conditions and constraints for the trajectory in-flight trajectory optimizations are as follows.
3. The initial path angle, initial speed, and initial altitude of Phase 1 are set to 89.9°, 10 m/s, and 0 m, respectively. At the Taiki-cho multipurpose park, the initial longitude and latitude are set to 143.44° east longitude and 42.50° north latitude, respectively, with the initial flight azimuth set to free.
4. The initial propellant mass is free, but a restriction is imposed on the maximum available propellant mass.
5. The engine is assumed to function only during Phase 1, and the throttle is set to between 0.5 and 1. Following that, the engine is turned off and the throttle is set to zero.
6. The angle of attack shall be limited to between − 20° and 30°.
7. At the end of Phase 2, the altitude must reach the target value, i.e., 120 km, as a constraint.
8. The return to the launch site is subject to specific constraints at the end of Phase 3. The terminal altitude must be at least 1000 m, the terminal path angle must be at least − 3°, and the terminal longitude and latitude must be the same as the launch site. The amount of propellant consumed should not be less than maximum amount of propellant that can be carried.

Since the overall design objectives explained in Sect. 4.1 are to minimize m_{lf} and to maximize h_{apogee} under the constraint that $m_{prop.f} \geq 0$, system-level objectives, F_1 and F_2, are written using a penalty-based constraint handling approach as follows:

$$\min. F_1 = m_{lf} - 1000 \min\left(m_{prop.f}, 0\right) \tag{1}$$

$$\min. F_2 = -0.1 h_{apogee} \tag{2}$$

The settings of MOEA/D are shown in Table 3. A desktop computer was used for optimization calculations.

Table 3 Setting of MOEA/D

Generation	30
Popular size	50
Niche size	5
Crossover method	Differential evolution (Scaling factor is 0.5)
Crossover ratio	1
Mutation method	Polynomial mutation ($\eta = 20$)
Mutation ratio	0.1

4.2 Design Analysis Models

100kN-class Liquid Oxygen/methane rocket engines, which are being studied by aerospace corporations, are installed in the engine performance model.

Hypersonic Aerospace Sizing Analysis (HASA) [17], developed by NASA, is used for vehicle mass analysis. HASA is a statistical estimation model that is based on existing data on space transportation. Inputting the airframe data and flight load conditions yields the masses of the airframe components. These masses are added together to obtain the dry mass of the aircraft.

Flight simulations are carried out using the aircraft's equations of motion in a three-degree-of-freedom mass point model. The trim condition is ignored in this optimization. The atmospheric model is based on the United States Standard Atmosphere 1976 [18], which specifies the atmospheric density, pressure, temperature, and sound velocity for each altitude. In the trajectory optimization calculation, a smooth atmospheric model is implemented by spline interpolation with each value. The equation of motion does not take into account the effect of the earth's rotation, but it does take into account the spherical shape of the earth.

5 Result and Discussions

5.1 Outline

It took 10 days to finish the computations by using a desktop computer with Intel Core i7 9700 CPU and 32 GB RAM. Figure 7 shows the Hypervolume values of the archived individuals in the optimization calculation. Figure 8 depicts the individuals' objective function values as determined by the optimization calculation. The Hypervolume value is almost coverging, and the evolution is assumed to have progressed sufficiently. The computation took three days up to 7 generations, and the computational cost was caused by the unstable initial computation. It has been identified that the load factor and total mass have an inverse relation. Solutions are searched towards the optimal lower-left direction while maintaining a high level of diversity, indicating that the optimization is effective.

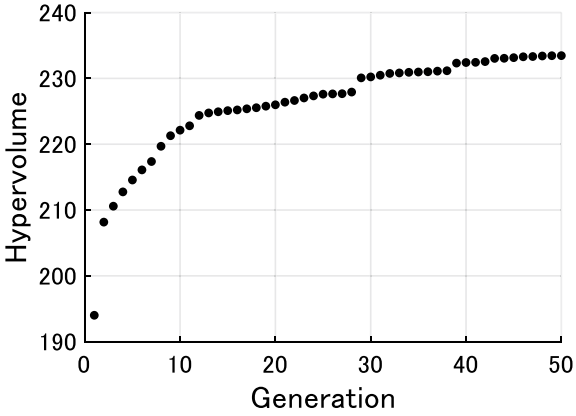

Fig. 7 Hypervolume

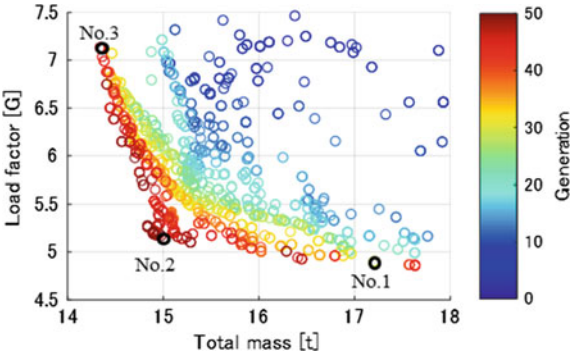

Fig. 8 All optimization solutions

5.2 Airframe and Trajectory

Table 4 shows the characteristics of typical solutions obtained in the optimization calculations.

Figures 9, 10, 11 depict typical optimization solutions' aircraft shape and flight trajectory. It was discovered that as the wing area grew larger and the initial mass increased, the load limit was reduced. Around 400 s into Solution No. 1's flight trajectory, the angle of attack becomes unstable. This output is because the continuity constraint is not strict, but it is not classified as an infeasible solution because it is considered to have little effect on the entire trajectory. When the wing area is reduced to near zero, the load factor rises and the propellant mass falls as the initial thrust-to-weight ratio rises. No.3's trajectory is omitted because its load factor is too large to be practical.

Table 4 Typical optimization solution specifications

Representative solution No		1	2	3
Body length	[m]	13.9	13.4	13.3
Root-chord length	[m]	6.35	4.67	4.61
Middle-chord length	[m]	4.42	1.46	1.14
Tip-chord length	[m]	0.96	1.31	1.08
Half span length	[m]	5.34	4.26	4.19
Main wing location	[m]	6.53	6.04	5.91
Maximum operating load factor	[G]	4.86	5.17	7.13
Maximum operating dynamic pressure	[kPa]	29,351	43,524	21,250
Initial thrust-to-weight ratio desired	[-]	1.27	1.21	1.60
The nozzle expansion ratio of engines	[-]	29.9	25.0	25.1
Sea level I_{sp}	[s]	341	338	338
Dry mass	[kg]	6230	5730	5870
Propellant mass	[kg]	11,400	9250	8470
Total mass	[kg]	17,600	15,000	14,300
Number of engines	[-]	3	2	3

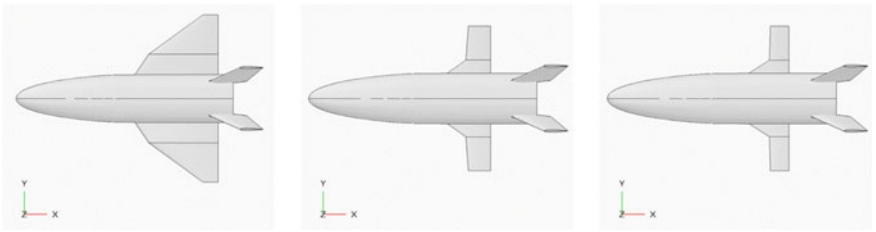

A) Solution No.1 B) Solution No.2 C) Solution No.3

Fig. 9 The airframe of typical optimization solutions

6 Conclusion

It was confirmed that the multi-fidelity surrogate model can evaluate aerodynamics with higher accuracy than the conventional low-accuracy aerodynamic evaluation method. Furthermore, it was confirmed that the model could be implemented in the MDO of suborbital spaceplanes and that optimization calculations could be performed successfully. The future work identified in this study are as follows.

- It is necessary to take into account of static stability and trim conditions in the trajectory calculation. This is because the trim condition is ignored in this optimization. In addition, it is necessary to estimate the aerodynamic characteristics of the shape with the elevon steering.

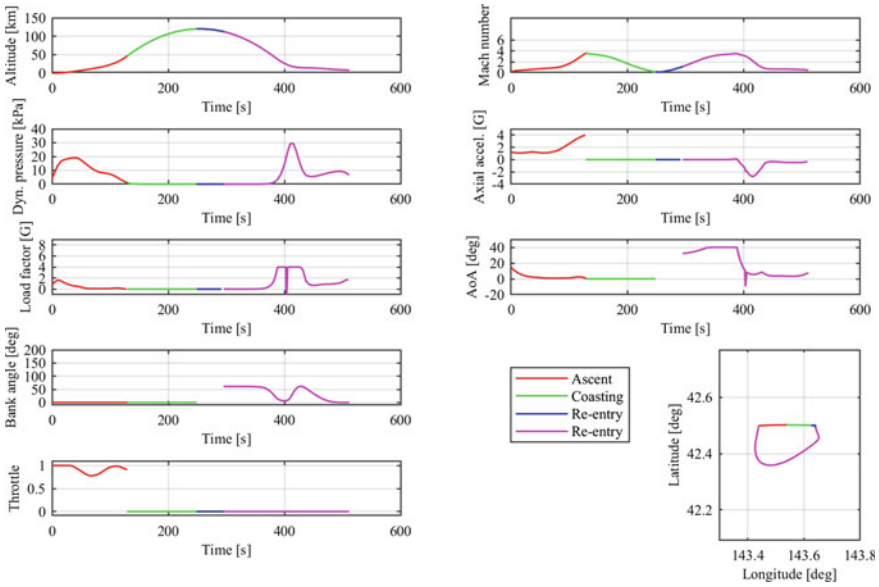

Fig. 10 Flight trajectory of Solution No.1

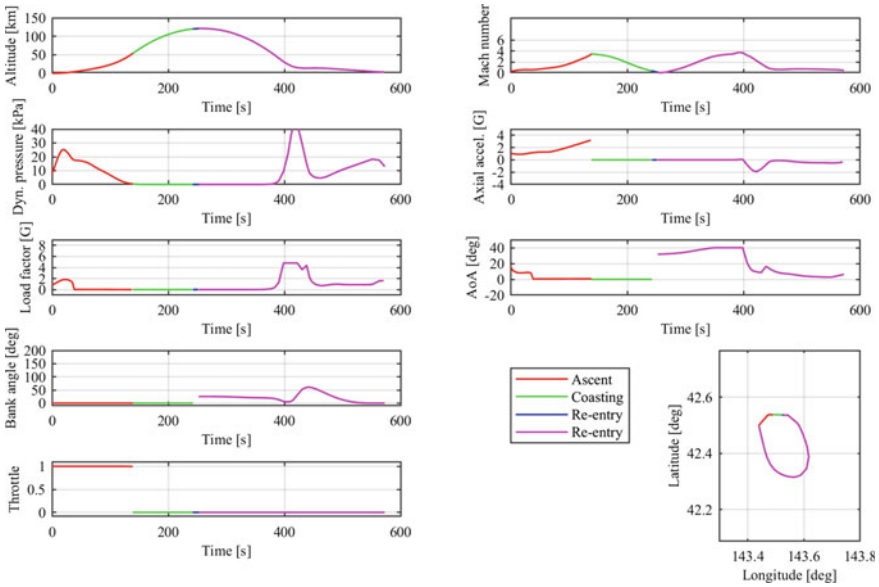

Fig. 11 Flight trajectory of Solution No.2

- The accuracy of the surrogate model for aerodynamics has been confirmed only for the HIMES geometry, and comparisons with other geometries are necessary.
- It is necessary to consider a trajectory calculation method that is stable in the initial generation of optimization.
- In this paper, the surrogate model of the aerodynamic characteristic evaluation method was constructed outside the optimization loop. However, when adding high-accuracy sample points, it is inefficient to do so randomly, and conducting CFD analysis in the loop can improve the solution's reliability. As a result, it is preferable to use MOEA/D-EGO.

References

1. Fujikawa T, Tsuchiya T, Tomioka S (2017) Multidisciplinary design optimization of a two-stage-to orbit reusable launch vehicle with ethanol-fueled rocket-based combined cycle engines. Trans Japan Soc Aeronaut Space Sci 60(5):265–275
2. Jones DR, Schonlau M, Welch WJ (1998) Efficient global optimization of expensive black-box functions. J Global Optim 13:455–492
3. Zhang Q, Liu W, Virginas B (2010) Expensive multiobjective optimization by MOEA/D with Gaussian process model. IEEE Trans Evolut Comput 14(3)
4. Li H, Zhang Q (2007) MOEA/D: a multiobjective evolutionary algorithm based on decomposition. IEEE Trans Evol Comput 11(6):712–731
5. Satterwhite CR (2015) Development of CPanel, an unstructured panel code, using a modified TLS velocity formulation. Master Thesis, California Polytechnic State University, San Luis Obispo
6. Hess RV, Gardner CS (1949) Study by the Prandtl-Glauert method of compressibility effects and critical mach number for ellipsoids of various aspect ratios and thickness ratios, NACATN-1792
7. Anderson JD (2006) Hypersonic and high-temperature gas dynamics (AIAA Education Series)
8. White FM (1974) Viscous fluid flow. McGraw-Hill, Inc., New York, NY, USA, p 639
9. Bonner E, Cloever W, Dunn K (1991) Aerodynamic preliminary analysis system II Part I—Theory. NASA CR-182076, p 58
10. Spalart PR (1992) A one-equation turbulence model for aero-dynamic flows. AIAA Paper 1992–439
11. Lei Z (2005) Effect of RANS turbulence models on computation of vertical flow over wing-body configuration. Trans. JSASS,48 pp 152–160
12. Forrester AIJ, Sóbester A, Keane AJ (2010) Multi-fidelity optimization via surrogate modelling. IEEE Transactions on Evol Comput 14(3)
13. Jones DR (2001) A taxonomy of global optimization methods based on response surfaces. J Global Optim 21:345–383
14. Forrester AIJ, Keane AJ, Bressloff NW (2006) Design and analysis of 'noisy' computer experiments. AIAA J 44:2331–2339
15. Kawaguchi J, Inatani Y, Yonemoto K, Hosokawa S (1987) On the flight control system of a winged space vehicle and physical simulation test. Institute of Space and Astronautical Science report 64:3–199
16. Li H, Zhang Q (2009) Multiobjective optimization problems with complicated pareto sets, MOEA/D and NSGA-II. IEEE Trans Evol Comput 13(2):284–302
17. Harloff GJ, Berkowitz BM (1988) HASA—hypersonic aerospace sizing analysis for the preliminary design of aerospace vehicles. NASA CR–182226
18. NOAA, NASA and U. A. Force (1976) U. S. Standard atmosphere. NASA TM-X-74335